Benchmarks for the ^{13}C NMR Chemical Shielding Tensors in Peptides in the Solid State

Jiř í Czernek, Tomasz Pawlak, Marek J. Potrzebowski

PII: S0009-2614(12)00041-3
DOI: 10.1016/j.cplett.2012.01.013
Reference: CPLETT 29961

To appear in: *Chemical Physics Letters*

Received Date: 23 November 2011
Accepted Date: 6 January 2012

Please cite this article as: J. Czernek, T. Pawlak, M.J. Potrzebowski, Benchmarks for the ^{13}C NMR Chemical Shielding Tensors in Peptides in the Solid State, *Chemical Physics Letters* (2012), doi: 10.1016/j.cplett.2012.01.013

Benchmarks for the ^{13}C NMR Chemical Shielding Tensors in Peptides in the Solid State

Jiří Czernek[1]*, Tomasz Pawlak[2], and Marek J. Potrzebowski[2]

[1]Institute of Macromolecular Chemistry

Academy of Sciences of the Czech Republic

Heyrovsky Square 2

162 06 Praha 6

The Czech Republic

Phone: +420-296809290. Fax: +420-296809410. Email: czernek@imc.cas.cz

[2] Centre of Molecular and Macromolecular Studies

Polish Academy of Sciences

Sienkiewicza 112

90 363 Łódź

Poland

* The author to whom the correspondence should be addressed.

Abstract

The benchmark set is proposed, which comprises 126 principal elements of chemical shielding tensors, and the respective isotropic chemical shielding values, of all 42 ^{13}C nuclei in crystalline Tyr-D-Ala-Phe and Tyr-Ala-Phe tripeptides with known, but highly dissimilar structures. These data are obtained by both the NMR measurements and the density functional theory in the pseudopotential plane-wave scheme. Using the CASTEP program, several computational strategies are employed, for which the level of agreement between calculations and experiment is established. This set is mainly intended for the validation of methods capable of predicting the ^{13}C NMR parameters in solid-state systems.

1. Introduction

Benchmark suites of molecules with reliable reference data are indispensable for the validation of computational methods, which exist already or will be developed, and also for parametrizations of approximate calculation strategies. Depending on the property to be predicted, various requirements are imposed upon the calibration sets (see, e.g., the accounts of benchmarking efforts for the energies of ground **[1]** and excited **[2]** electronic states). Vastly varying are also the collections of molecules for testing the methods, which treat the parameters related to the nuclear magnetic resonance (NMR) chemical shielding property (see ref. **[3]** for definitions). Thus, the isotropic chemical shifts of small molecules were benchmarked **[4]**, **[5]** against the values measured using the gas-phase NMR experiments **[6]**. In addition, all six independent components of chemical shielding tensors **[7]** obtained by the single-crystal solid-state NMR techniques **[8]** were employed in the validation of methods, which differ in the treatment of the condensed phase surrounding the investigated single crystals **[9]**, **[10]**. Unfortunately, no extensive benchmarks were reported for the theoretical predictions of solvent effects upon the chemical shifts **[11]**. As for the chemical shielding parameters, which can be determined from the magic-angle-spinning solid-state (MAS SS) NMR experiments on powder samples **[3]**, i.e., the isotropic chemical shift and the principal components of the chemical shielding tensor, perhaps the most important testing molecules are amino acids (see **[12]**, **[13]**, **[14]** and references cited therein) due to their pronounced significance for biomolecular NMR explorations **[15]**. The smallest units composed of amino acids, i.e., dipeptides, were systematically studied by joint experimental/computational efforts to reveal the trends in the above-mentioned NMR data as functions of geometrical parameters relevant for the structure of proteins (for a review, see ref. **[16]**). Larger peptides are also becoming treated by the combination of MAS SS NMR measurements and quantum chemical methods of varying degree of sophistication (cf. references **[17]**, **[18]**). Such investigations,

which are expected to be crucial in the evolving area of NMR crystallography **[19]**, clearly need the benchmarks against which the various computational protocols could be compared. Hence, for two crystalline tripeptides with previously resolved **[20]**, **[21]**, by quite different crystals structures, the set of 42 ^{13}C isotropic chemical shifts and 126 principal elements of the ^{13}C chemical shift tensors was experimentally established by the MAS SS NMR, and is compared in this Letter to the data predicted using the method for first-principles calculations of geometries and NMR parameters in periodic systems. Thus, the combination of the density functional theory (DFT) and the plane-wave pseudopotential approach (see Methods) is employed to test the reliability of various computational schemes.

2. Methods

The compounds Tyr-D-Ala-Phe and Tyr-Ala-Phe (i.e., two tripeptides differing in the chirality of alanine) were investigated. They will be further referred to as peptides **1** and **2**, respectively. Their biological significance, preparation, and X-ray diffraction (XRD) studies were described in references **[20]** and **[21]** accordingly. The samples of **1** and **2** were subjected to the cross-polarization MAS SS NMR measurements of the ^{13}C isotropic chemical shifts, which were assigned with the aid of the liquid-state NMR experiments (cf. **[20]**). Subsequently the 2D-PASS experiments **[22]** were carried out, and the eigenvalues of the chemical shift tensors of all the carbon atoms were obtained by the standard procedure of fitting the sideband manifolds to the spectra **[23]**. The full account of the NMR measurements is given elsewhere **[24]**. Both peptides **1** and **2** comprise 21 nonequivalent carbons, with the numbering defined in the Supporting Information files (222456.PDB and 720512.PDB). It should be noted that this numbering differs from that of the corresponding CIF files, which are deposited in the Cambridge Structural Database **[25]**. Resulting 126 experimental principal components of the ^{13}C chemical shift tensors are supplied as the commented

Matlab® file Tensors.M in the Supporting Information, in the form of a row-vector complying with the present numbering of atoms. Hopefully, this format enables the straightforward comparison of measured values with their predicted counterparts, not restricted to the calculations performed here. The latter can be divided into three groups. The first one entails the direct application of the experimental X-ray structures of **1** and **2**, while for the remaining two groups the geometrical optimizations were carried out using the approach, which provides for a realistic solid-state treatment of crystalline systems, and whose details can be found in references **[26]**, **[27]** and **[28]**. Thus, the constrained (with only the positions of hydrogens allowed to vary) and full (adjusting the positions of all atoms) lattice-energy minimizations were performed by applying the "Fine" level of settings in the CASTEP program **[29]**. In all three types of calculations, the lattice parameters were fixed to their experimental values **[20]**, **[21]**, and the generalized density approximation DFT functionals PBE **[30]**, PW91 **[31]** and RPBE ("revised PBE") **[32]** were respectively adopted. Hence, for the peptides **1** and **2**, nine geometries were considered. For each of them, the chemical shielding tensors of all the atoms in the unit cell with applied periodic boundary conditions were obtained by means of the gauge-including projector augmented-wave (GIPAW) computations **[33]**, **[34]**. Again, the "Fine" defaults of CASTEP were adopted, and nine sets of the GIPAW results were obtained, because the same above-mentioned DFT functionals were used for the NMR calculations as for the treatment of the geometries. Additionally, using Gaussian 03 suite of quantum chemical programs **[35]**, the positions of only the hydrogen atoms in isolated structures of **1** and **2** were optimized by combining the B3LYP **[36]**, **[37]** DFT functionals with the standard 6-311G** basis set, and the chemical shielding tensors were subsequently obtained by the GIAO-B3LYP/TZ2P **[38]**, **[39]** approach, which successfully described NMR parameters in a number of systems **[40]**, **[41]**, **[42]**. Only the absolute values of principal components of the ^{13}C chemical shielding tensors, σ_{xx}, σ_{yy}, σ_{zz},

and of the ^{13}C isotropic chemical shielding σ^{iso}, $\sigma^{iso} = (\sigma_{xx} + \sigma_{yy} + \sigma_{zz})/3$, were considered, i.e., no referencing to the experimental shielding scale **[3]** was attempted, for the reasons described in Part 3.1. Thus, the linear relationships between these data and their experimental chemical shift counterparts were described by least-squares fits of two parameters, *a* and *b*, to the simple functional form

$$y = a*x + b \quad (1)$$

where *y* and *x* denote the chemical shielding and chemical shift values, respectively (in a hypothetical case of the perfect agreement between theory and measurements, the slope, *a*, should equal to –1.0, and the intercept, *b*, would represent the true value of the absolute chemical shielding of the chosen nucleus in a reference compound). All the calculated results, which were statistically evaluated using the Origin® software, are available in plain-text format as the Supporting Information file Tensors.dat.

3. Results and Discussion

3.1 An Overall Agreement between Calculated and Measured Data

Table 1

Table 2

Tables 1 and 2 summarize the statistical data relevant for the comparison of the theoretical ^{13}C chemical shielding tensors and ^{13}C isotropic chemical shielding with the corresponding experimental ^{13}C chemical shifts of the respective tripeptides. Much better agreement was achieved for the isotropic data. This is not surprising, as they represent the average value of the principal components and the errors in calculating the latter often compensate each other (see, e.g., ref. **[43]**). One important example will briefly be described here. The phenyl ring of

the phenylalanine moiety in Tyr-D-Ala-Phe was found to be highly flexible (in contrary to the same ring in the Tyr-Ala-Phe, and to the phenol rings of tyrosine in both peptides **1** and **2**) **[20]**. Of course, this type of motion(s), analyzed in detail in ref. **[24]**, is not taken into account by the present calculations properly (only indirectly, to the extent by how the crystal structure is influenced as a whole). This leads to large errors (sometimes exceeding 50 ppm) in the predicted principal elements of the ^{13}C chemical shielding tensors of the aromatic carbon atoms involved. However, the isotropic chemical shielding of those atoms is affected by about 2 – 3 ppm only, i.e., much less than might be expected on the basis of errors in the individual tensor components. This is illustrated in Figure 1, which shows the differences between the fitted (Equation 1) and calculated (using the PBE functional for both the full geometrical optimization and chemical shielding computations) values for the least shielded tensors component, denoted as σ_{xx}, together with this data for the negative of the sum of the remaining two principal elements, $-(\sigma_{yy} + \sigma_{zz})$. Four carbon atoms from the aromatic region of phenylalanine in the peptide **1** (marked as squares) and **2** (circles) are presented, and the dotted line corresponds to a situation of the complete error cancellation. The absolute values of these differences are much smaller for **2** than for **1**, however, the sum of all three components does not exceed 9 ppm for any of the eight atoms considered, which means the errors in predicted isotropic shielding are all smaller than 3 ppm for both peptides. As a consequence, the problems associated with predicting the chemical shielding, as those caused by the segmental dynamics of the phenyl ring in **1**, could remain undetected if only the isotropic values were considered. In fact, it was repeatedly shown (most recently for the polymorphs of piroxicam **[44]**) that for the characterization of crystalline compounds the full tensorial information is much more suitable (but more difficult to obtain, though) than the isotropic chemical shifts.

Figure 1

Table 3 collects the statistical analysis of the linear correlations of the ^{13}C chemical shielding data, which were calculated for both peptides **1** and **2**, with the experimental results. Figure 2 illustrates the level of agreement between theory and measurements achieved by the most reliable approach from those considered here (cf. Table 3), i.e., an application of the PBE functional for both the full geometrical optimization and chemical shielding computations. Some points in Figure 2 are immediately seen to be highly distant, by more than one standard deviation of the model expressed by Equation (1), from the fitted line. However, those "outliers" describe the chemical shielding of the aromatic carbons of phenylalanine in **1**, which are influenced strongly by the dynamic disorder **[24]**. Hence, without an adoption of the motional model(s) **[45]**, they should not be expected to be correctly predicted by the calculations. Indeed, if the 36 principal elements of respective chemical shielding tensors are removed from the benchmark set, the average absolute deviation drops to 4.2 ppm only (to be compared to an estimated ±3 ppm experimental uncertainty in these values). If they are kept, however, they could serve as the check of a fortuitous cancellation of errors is some method(s), leading to an accidental agreement with experiment.

Table 3

Figure 2

It is remarked that the measured values are compared directly to the computed ones, without first establishing "a theoretical shielding scale" and later converting the calculated chemical shielding to chemical shift data for a subsequent comparison with experimental values, so that the statistical analysis is not biased by introducing the influence of an inadequate treatment of standards (in the MAS SS NMR experiments, a secondary chemical shift reference is used **[46]**). It should be kept in mind that errors in the prediction of absolute chemical shielding

values in general differ between the reference and target compounds, and some statistical parameters are influenced by this inconsistency (see ref. **[47]** for in-depth discussion). Nevertheless, using the recommended value of 170.9 ppm **[13]**, **[14]**, the ^{13}C chemical shielding data calculated by the GIPAW approach can be immediately converted to the experimental carbon chemical shift scale referenced to liquid tetramethylsilane at room temperature. As Figure 3 demonstrates, this conversion works very well for the PBE results described above, producing the intercept of the linear reliationship between the theoretical and measured chemical shifts of –0.50 ppm only.

Figure 3

3.2 Geometry Optimizations and the Selection of DFT Functionals

The results in Tables 1 – 3 can be divided into two types of dependences, one describing the role of geometry optimizations, the other related to the choice of exchange-correlation functional for the calculations. Thus, for all three types of structures, i.e., subjected to the full, constrained and no optimization, the DFT functionals applied here do not differ substantially in the quality of the predicted ^{13}C chemical shielding data. Numerical instabilities reported for the PW91 calculations **[48]** were not observed. In fact, the GIPAW PW91 results, which were obtained for the isotropic chemical shielding of the PW91 optimized structure of **2** (cf. Table 2), appear to show the best agreement (judged by the values of parameters describing the least-squares fits) with experiment from all the approaches considered. Much more dramatic are the differences brought about by the treatment of the geometries of peptides **1** and **2**. Interestingly, the GIAO-BLYP/TZ2P results predicted for isolated molecules after their partial optimization (cf. Methods) are of similar quality as the GIPAW data obtained for unoptimized crystal structures (but the accuracy of both procedures is fairly low, see Tables 1 – 3). This finding likely suggests that the ^{13}C chemical shielding tensors are less sensitive to

their environment (the solid-phase structure) than to the hydrogen positions within the molecule. Nonetheless, an application of the periodic structure model to both the structural optimization and to the prediction of chemical shielding parameters is required for an almost quantitative agreement between the latter and experiment. As follows from an inspection of Tables 1 – 3, in the case of the isotropic chemical shielding in peptides **1** and **2**, the geometries need to be fully optimized to reduce the average and maximum discrepancies between theory and measurements to ca. one and three ppm, respectively. Considering all the limitations of the GIPAW DFT calculations for essentially static structures, these values are probably as low as can be currently achieved (see also the discussion in references **[10]** and **[47]**). However, the geometry optimization might even partially compensate for an inconsistency of XRD and NMR measurements, which were carried out at vastly differing temperatures **[20]**, **[21]**. In contrast to the isotropic chemical shielding, the type of structural optimization (full or limited to the hydrogen nuclei) influences only mildly the agreement between theory and experiment for principal elements of chemical shielding tensors in **1** and **2**. The level of agreement thus achieved approaches the ±3 ppm accuracy of measuring these data (of course, this does not hold for carbons in the mobile fragment as described in Part 3.1).

4. Conclusions

The benchmark set is proposed comprising 126 principal elements of chemical shielding tensors, and the respective isotropic chemical shielding values, of all 42 ^{13}C nuclei in crystalline Tyr-D-Ala-Phe and Tyr-Ala-Phe tripeptides. Their structures, established previously by the XRD technique, differ significantly in the conformation, crystal packing, and dynamics **[24]**. The ^{13}C chemical shielding parameters are obtained by both the MAS SS NMR measurements and the DFT GIPAW calculations. The statistical evaluation of the

agreement between the results from several computational schemes (also including the GIAO calculations on isolated molecules) and experiment is presented. This provides for the reference data for comparison with the results of ^{13}C chemical shielding predictions and for possibly improving the empirical models **[9]**.

Acknowledgements

This work was supported by the Ministry of Education, Youths and Sports of the Czech Republic (MŠMT 2B08021) and by the National Center of Sciences, Poland (DEC-2011/01/N/ST4/03108). We are grateful to Dr. Michal Hušák, Institute of Chemical Technology in Prague, for the technical assistance with CASTEP calculations.

References

[1] T. Helgaker, P. Jørgensen, J. Olsen, Molecular Electronic Structure Theory, Wiley, Chichester, 2001.

[2] R. Send, M. Kühn, F. Furche, J. Chem. Theory Comput. 7 (2011) 2376.

[3] M. J. Duer, Introduction to Solid-State NMR Spectroscopy, Blackwell, Oxford, 2004.

[4] A. A. Auer, J. Gauss, J. F. Stanton, J. Chem. Phys. 118 (2003) 10407.

[5] Y. Zhao, D. G. Truhlar, J. Phys. Chem. A 112 (2008) 6794.

[6] C. J. Jameson, Chem. Rev. 91 (1991) 1375.

[7] T. H. Sefzik, D. Turco, R. J. Iuliucci, J. C. Facelli, J. Phys. Chem. A 109 (2005) 1180.

[8] M. H. Sherwood, D. W. Alderman, D. M. Grant, J. Mag. Res. 84 (1989) 466.

[9] A. M. Orendt, J. C. Facelli, in: G. A. Webb (Ed.), Annual Reports on NMR Spectroscopy, Academic Press, New York, 2007, p. 115.

[10] J. C. Johnston, R. J. Iuliucci, J. C. Facelli, G. Fitzgerald, K. T. Mueller, J. Chem. Phys. 131 (2009) Art. No. 144503.

[11] A. Bagno, F. Rastrelli, G. Saielli, Chem.-Eur. J. 12 (2006) 5514.

[12] R. H. Havlin, H. B. Le, D. D. Laws, A. C. deDios, E. Oldfield, J. Am. Chem. Soc. 119 (1997) 11951.

[13] C. Gervais, R. Dupree, K. J. Pike, C. Bonbomme, M. Profeta, C. J. Pickard, F. Mauri, J. Phys. Chem. A 109 (2005) 6960.

[14] A. Zheng, S.-B. Liu, F. Deng, J. Comput. Chem. 30 (2009) 222.

[15] J. Cavanagh, W. J. Fairbrother, A. G. Palmer III, M. Rance, N. J. Skeleton, Protein NMR Spectroscopy, Elsevier Academic Press, Burlington, MA, 2007.

[16] D. Mukkamala, Y. Zhang, E. Oldfield, J. Am. Chem. Soc. 129 (2007) 7385.

[17] I. De Gortari, G. Portella, X. Salvatella, V. S. Bajaj, P. C. A. van der Wel, J. R. Yates, M. D. Segall, C. J. Pickard, M. C. Payne, M. Vendruscolo, J. Am. Chem. Soc. 132 (2010) 5993.

[18] L. Rougier, A. Milon, V. Reat, F. Jolibois, Phys. Chem. Chem. Phys. 12 (2010) 6999.

[19] R. K. Harris, R. E. Wasylishen, M. J. Duer, NMR Crystallography, Wiley, Chichester, 2010.

[20] M. M. Słabicki, M. J. Potrzebowski, G. Bujacz, S. Olejniczak, J. Olczak, J. Phys. Chem. B 108 (2004) 4535.

[21] K. Trzeciak-Karlikowska, A. Bujacz, A. Jeziorna, W. Ciesielski, G. D. Bujacz, J. Gajda, D. Pentak, M. J. Potrzebowski, Cryst. Growth Des. 9 (2009) 4051.

[22] O. N. Antzutkin, S. C. Shekar, M. H. Levitt, J. Mag. Res. 115 (1995) 7.

[23] M. Bak, J. T. Rasmussen, N. C. Nielsen, J. Mag. Res. 147 (2000) 296.

[24] T. Pawlak, K. Trzeciak-Karlikowska, J. Czernek, W. Ciesielski and M. J. Potrzebowski, J. Phys. Chem. B (2011) submitted.

[25] F. H. Allen, Acta Cryst. B 58 (2002) 380.

[26] G. Kresse, D. Joubert, Phys. Rev. B 59 (1999) 1758.

[27] M. D. Segall, P. J. D. Lindan, M. J. Probert, C. J. Pickard, P. J. Hasnip, S. J. Clark, M. C. Payne, J. Phys. Condens. Mat. 14 (2002) 2717.

[28] P. Gianozzi, S. Baroni, N. Bonini, et al., J. Phys. Condens. Mat. 21 (2009) Art. No. 395502.

[29] S. J. Clark, M. D. Segall, C. J. Pickard, P. J. Hasnip, M. J. Probert, K. Refson, M. C. Payne, Z. Kristallogr. 220 (2005) 567.

[30] J. P. Perdew, K. Burke, K., M. Ernzerhof, Phys. Rev. Lett. 77 (1996) 3865.

[31] J. P. Perdew, Y. Wang, Phys. Rev. B 33 (1986) 8800.

[32] B. Hammer, L. B. Hansen, J. K. Norskov, Phys. Rev. B 59 (1999) 7413.

[33] C. J. Pickard, F. Mauri, Phys. Rev. B 63 (2001) Art. No. 245101.

[34] J. R. Yates, C. J. Pickard, F. Mauri, Phys. Rev. B 76 (2007) Art. No. 024401.

[35] M. J. Frisch, G. W. Trucks, H. B. Schlegel et al., Gaussian 03, Revision C.02, Gaussian, Inc., Wallingford, CT, 2004.

[36] A. D. Becke, J. Chem. Phys. 98 (1993) 5648.

[37] C. Lee, W. Yang, R. Parr, Phys. Rev. B 37 (1998) 785.

[38] K. Wolinski, J. F. Hinton, P. Pulay, J. Am. Chem. Soc. 112 (1990) 8251.

[39] A. Schäfer, H. Horn, R. Ahlrichs, J. Chem. Phys. 97 (1992) 2571.

[40] J. Czernek, J. Phys. Chem. A 105 (2001) 1357.

[41] J. Czernek, J. Phys. Chem. A 107 (2003) 3952.

[42] J. Czernek, Chem. Phys. Lett. 392 (2004) 508.

[43] A. C. deDios, E. Oldfield, Solid State Nucl. Mag. 6 (1996) 101.

[44] W. Liu, W. D. Wang, W. Wang, S. Bai, C. Dybowski, J. Phys. Chem. B 114 (2010) 16641.

[45] J. Lorieau, A. E. McDermott, Magn. Reson. Chem. 44 (2006) 334.

[46] C. R. Morcombe, K. W. Zilm, J. Mag. Res. 162 (2003) 479.

[47] R. K. Harris, P. Hodgkinson, C. J. Pickard, J. R. Yates, V. Zorin, Magn. Reson. Chem. 45 (2007) S174.

[48] M. Benoit, M. Profeta, F. Mauri, C. J. Pickard, M. E. Tuckerman, J. Phys. Chem. B 109 (2005) 6052.

Figure 1. The compensation of the predicted ^{13}C chemical shielding differences. See the text for details.

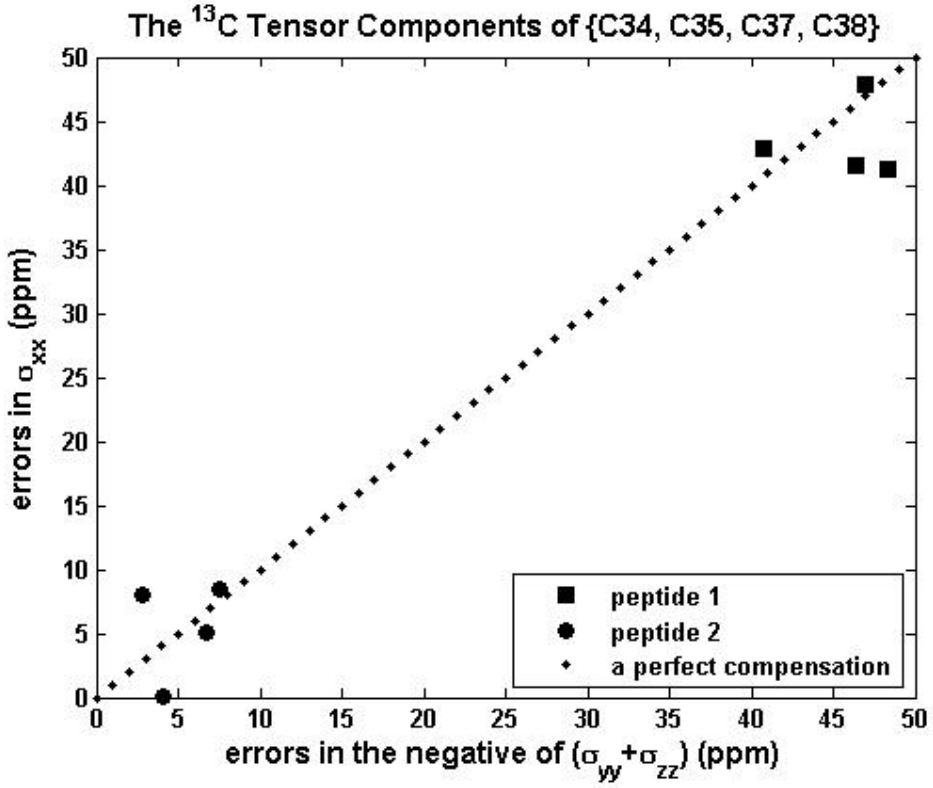

Figure 2. The comparison of the experimental ^{13}C chemical shielding with the GIPAW PBE results. See the text for details.

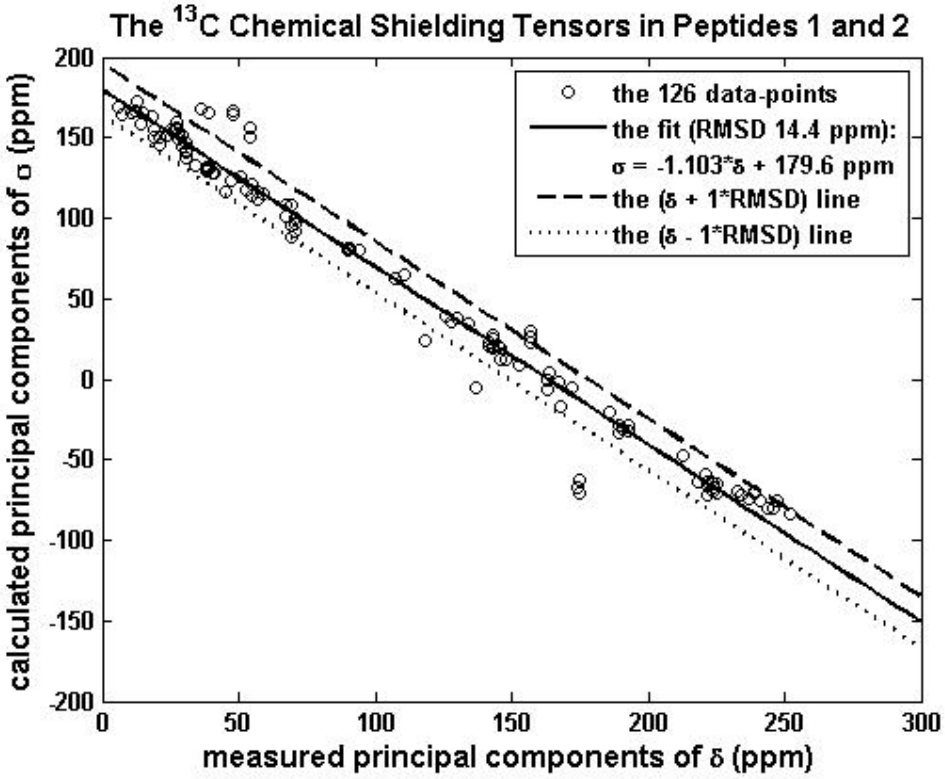

Figure 3. The comparison of the experimental ^{13}C chemical shifts with the GIPAW PBE results obtained by subtracting the calculated absolute isotropic shielding from the value of 170.9 ppm. See the text for details.

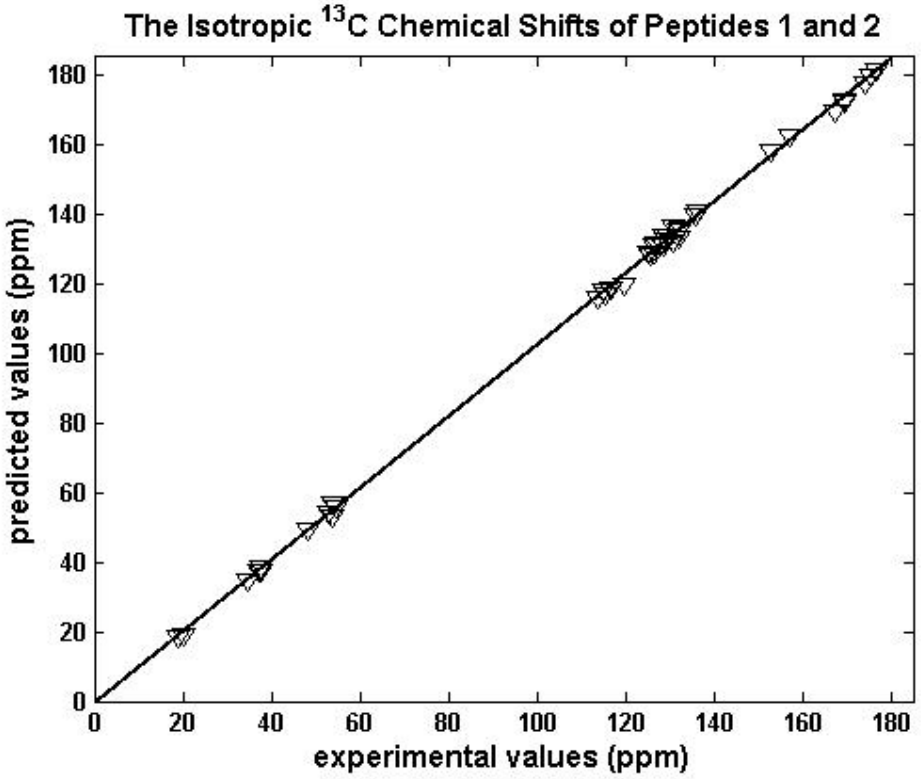

Table 1. The statistical evaluation of an agreement between predicted ^{13}C NMR data and their counterparts established experimentally for Tyr-D-Ala-Phe. The results for the 21 isotropic chemical shieldings/shifts and (in parentheses) the 63 principal elements of chemical shielding/shift tensors are shown. See the text for details.

functional	geometry	slope	standard error of slope	intercept (ppm)	standard error of intercept (ppm)	standard deviation (ppm)	average absolute deviation (ppm)	maximum absolute deviation (ppm)	adjusted R^2
PBE	fully optimized	–1.0304 (–1.133)	0.0056 (0.033)	171.50 (182.8)	0.67 (4.4)	1.16 (19.3)	0.93 (13.2)	2.12 (54.7)	0.99941 (0.95000)
	hydrogens relaxed	–1.0105 (–1.117)	0.0094 (0.034)	171.11 (182.8)	1.12 (4.5)	1.96 (19.7)	1.60 (13.8)	3.93 (57.1)	0.99827 (0.94663)
	not optimized	–1.1419 (–1.215)	0.0228 (0.035)	191.13 (199.1)	2.72 (4.7)	4.74 (20.6)	3.91 (15.0)	10.89 (62.4)	0.99208 (0.95065)
PW91	fully optimized	–1.0283 (–1.131)	0.0079 (0.033)	171.16 (182.4)	0.94 (4.4)	1.65 (19.5)	1.36 (13.7)	3.25 (54.4)	0.99881 (0.94888)
	hydrogens relaxed	–1.0090 (–1.115)	0.0091 (0.034)	170.84 (182.5)	1.09 (4.5)	1.90 (19.7)	1.56 (13.8)	3.76 (56.9)	0.99836 (0.94664)
	not optimized	–1.1226 (–1.238)	0.0221 (0.038)	192.14 (204.8)	2.63 (5.1)	4.59 (22.4)	3.82 (16.1)	10.75 (57.8)	0.99234 (0.94412)
RPBE	full optimized	–1.0183 (–1.120)	0.0078 (0.033)	172.20 (183.4)	0.93 (4.4)	1.63 (19.3)	1.35 (13.6)	3.41 (54.2)	0.99882 (0.94921)
	hydrogens relaxed	–0.9979 (–1.102)	0.0089 (0.033)	172.65 (184.1)	1.06 (4.4)	1.85 (19.4)	1.53 (13.6)	3.71 (56.6)	0.99841 (0.94694)
	not optimized	–1.1258 (–1.197)	0.0225 (0.035)	192.08 (199.9)	2.68 (4.6)	4.67 (20.2)	3.81 (14.8)	10.80 (61.6)	0.99210 (0.95085)
B3LYP[a]	hydrogens relaxed[b]	–0.9923 (–1.115)	0.0239 (0.037)	178.22 (191.7)	2.85 (4.9)	4.96 (21.7)	4.11 (15.0)	10.09 (59.3)	0.98857 (0.93613)

Captions to Table 1:

[a] Combined with the GIAO approach and the TZ2P **[39]** basis set.

[b] The B3LYP/6-311G** constrained optimization of an isolated molecule.

Table 2. The statistical evaluation of an agreement between predicted ^{13}C NMR data and their counterparts established experimentally for Tyr-Ala-Phe. The results for the 21 isotropic chemical shieldings/shifts and (in parentheses) the 63 principal elements of chemical shielding/shift tensors are shown. See the text for details.

functional	geometry	slope	standard error of slope	intercept (ppm)	standard error of intercept (ppm)	standard deviation (ppm)	average absolute deviation (ppm)	maximum absolute deviation (ppm)	adjusted R^2
PBE	fully optimized	–1.0266 (–1.077)	0.0057 (0.009)	171.31 (176.8)	0.69 (1.3)	1.19 (6.0)	0.85 (4.8)	2.73 (13.8)	0.99938 (0.99523)
	hydrogens relaxed	–1.0025 (–1.055)	0.0121 (0.010)	173.04 (178.8)	1.45 (1.3)	2.52 (6.2)	1.85 (4.9)	5.95 (16.9)	0.99712 (0.99470)
	not optimized	–1.1197 (–1.176)	0.0177 (0.014)	192.72 (198.9)	2.13 (1.9)	3.71 (8.9)	3.18 (7.1)	6.17 (24.0)	0.99501 (0.99115)
PW91	fully optimized	–1.0251 (–1.075)	0.0055 (0.009)	171.03 (176.6)	0.66 (1.2)	1.15 (5.7)	0.88 (4.5)	2.55 (13.7)	0.99943 (0.99573)
	hydrogens relaxed	–1.0014 (–1.054)	0.0120 (0.010)	172.87 (178.6)	1.44 (1.3)	2.51 (6.2)	1.90 (4.9)	6.08 (16.7)	0.99715 (0.99473)
	not optimized	–1.1322 (–1.143)	0.0264 (0.016)	190.86 (192.1)	3.17 (2.2)	5.51 (10.6)	4.26 (7.8)	13.21 (26.5)	0.98928 (0.98817)
RPBE	full optimized	–1.0125 (–1.064)	0.0060 (0.009)	171.77 (177.5)	0.73 (1.2)	1.26 (5.5)	1.01 (4.6)	2.66 (12.6)	0.99929 (0.99581)
	hydrogens relaxed	–0.9898 (–1.041)	0.0120 (0.009)	174.53 (180.2)	1.44 (1.3)	2.50 (5.9)	1.87 (4.8)	5.98 (15.2)	0.99709 (0.99498)
	not optimized	–1.1035 (–1.159)	0.0176 (0.014)	193.56 (199.7)	2.11 (1.9)	3.69 (8.7)	3.14 (7.0)	6.27 (22.4)	0.99492 (0.99126)
B3LYP[a]	hydrogens relaxed[b]	–0.9919 (–1.053)	0.0220 (0.017)	180.78 (187.5)	2.64 (2.3)	4.60 (10.5)	3.57 (7.9)	11.05 (31.5)	0.99026 (0.98483)

Captions to Table 2:

[a] Combined with the GIAO approach and the TZ2P **[39]** basis set.

[b] The B3LYP/6-311G** constrained optimization of an isolated molecule.

Table 3. The statistical evaluation of an agreement between predicted ^{13}C NMR data and their counterparts established experimentally for Tyr-D-Ala-Phe and Tyr-Ala-Phe. The results for the 42 isotropic chemical shieldings/shifts and (in parentheses) the 126 principal elements of chemical shielding/shift tensors are shown. See the text for details.

functional	geometry	slope	standard error of slope	intercept (ppm)	standard error of intercept (ppm)	standard deviation (ppm)	average absolute deviation (ppm)	maximum absolute deviation (ppm)	adjusted R^2
PBE	fully optimized	–1.0284 (–1.103)	0.0039 (0.017)	171.41 (179.6)	0.47 (2.2)	1.17 (14.4)	0.91 (8.6)	2.83 (56.9)	0.99940 (0.97227)
	hydrogens relaxed	–1.0062 (–1.083)	0.0089 (0.017)	172.05 (180.6)	1.06 (2.3)	2.65 (14.8)	2.04 (9.0)	7.38 (60.8)	0.99682 (0.96973)
	not optimized	–1.1304 (–1.194)	0.0157 (0.018)	191.88 (198.9)	1.88 (2.5)	4.70 (16.0)	3.93 (10.7)	9.71 (65.8)	0.99212 (0.97091)
PW91	fully optimized	–1.0267 (–1.101)	0.0047 (0.017)	171.09 (179.3)	0.56 (2.3)	1.41 (14.5)	1.12 (8.7)	3.26 (56.5)	0.99914 (0.97201)
	hydrogens relaxed	–1.0050 (–1.082)	0.0088 (0.017)	171.83 (180.3)	1.06 (2.3)	2.64 (14.8)	2.02 (9.0)	7.53 (60.6)	0.99685 (0.96974)
	not optimized	–1.1276 (–1.187)	0.0172 (0.020)	191.53 (198.1)	2.1 (2.8)	5.15 (17.7)	4.07 (11.7)	14.42 (59.9)	0.99051 (0.96423)
RPBE	fully optimized	–1.0154 (–1.090)	0.0049 (0.017)	171.98 (180.2)	0.58 (2.2)	1.45 (14.3)	1.18 (8.7)	3.52 (56.3)	0.99907 (0.97213)
	hydrogens relaxed	–0.9936 (–1.069)	0.0087 (0.017)	173.56 (181.9)	1.04 (2.3)	2.59 (14.5)	1.98 (8.8)	7.39 (60.1)	0.99689 (0.97003)
	not optimized	–1.1142 (–1.176)	0.0155 (0.018)	192.78 (199.6)	1.86 (2.4)	4.64 (15.7)	3.84 (10.6)	9.66 (64.9)	0.99210 (0.97107)
B3LYP[a]	hydrogens relaxed[b]	–0.9918 (–1.082)	0.0164 (0.020)	179.47 (189.4)	1.97 (2.7)	4.91 (17.2)	4.02 (11.5)	11.42 (62.8)	0.98890 (0.95963)

Captions to Table 3:

[a] Combined with the GIAO approach and the TZ2P **[39]** basis set.

[b] The B3LYP/6-311G** constrained optimization of an isolated molecule.

The benchmark set for the ^{13}C NMR chemical shielding parameters in the solid state. Values in two tripeptides measured and calculated by a number of DFT approaches. State-of-the-art data for 126 principal elements of ^{13}C chemical shielding tensors.